International Journal of Nanomedicine

Dovepress
open access to scientific and medical research

Open Access Full Text Article

ORIGINAL RESEARCH

Praziquantel–lipid nanocapsules: an oral nanotherapeutic with potential *Schistosoma mansoni* tegumental targeting

This article was published in the following Dove Press journal:
International Journal of Nanomedicine

Rokaya O Amara[1,2]
Alyaa A Ramadan[1]
Riham M El-Moslemany[1]
Maha M Eissa[3]
Mervat Z El-Azzouni[3]
Labiba K El-Khordagui[1]

[1]Department of Pharmaceutics, Faculty of Pharmacy, Alexandria University, Alexandria, Egypt; [2]Biotechnology Research Center, Tripoli, Libya; [3]Department of Medical Parasitology, Faculty of Medicine, Alexandria University, Alexandria, Egypt

Purpose: Lipid nanocapsules (LNCs) have shown potential to increase the bioavailability and efficacy of orally administered drugs. However, their intestinal translocation to distal target sites and their implication in pharmacokinetic (PK)–pharmacodynamic (PD) relationships are yet to be elucidated. In this study, the effect of LNCs on the PD activity and pharmacokinetics of praziquantel (PZQ), the mainstay of schistosomiasis chemotherapy, was investigated.

Materials and methods: The composition of LNCs was modified to increase PZQ payload and to enhance membrane permeability. PZQ–LNCs were characterized in vitro for colloidal properties, entrapment efficiency (EE%), and drug release. PD activity of the test formulations was assessed in *Schistosoma mansoni*-infected mice 7 days post-oral administration of a single 250 mg/kg oral dose. Pharmacokinetics of the test formulations and their stability in simulated gastrointestinal (GI) fluids were investigated to substantiate in vivo data.

Results: PZQ–LNCs exhibited good pharmaceutical attributes in terms of size (46–62 nm), polydispersity index (0.01–0.08), EE% (>95%), and sustained release profiles. Results indicated significant efficacy enhancement by reduction in worm burden, amelioration of liver pathology, and extensive damage to the fluke suckers and tegument. This was partly explained by PK data determined in rats. In addition, oral targeting of the worms was supported by the stability of PZQ–LNCs in simulated GI fluids and scanning electron microscopy (SEM) visualization of nanostructures on the tegument of worms recovered from mesenteric/hepatic veins. Cytotoxicity data indicated tolerability of PZQ–LNCs.

Conclusion: Data obtained provide evidence for the ability of oral LNCs to target distal post-absorption sites, leading to enhanced drug efficacy. From a practical standpoint, PZQ–LNCs could be suggested as a potential tolerable single lower dose oral nanomedicine for more effective PZQ mass chemotherapy.

Keywords: lipid nanocapsules, praziquantel, *Schistosoma mansoni*, bioavailability, oral targeting, pharmacokinetics, tegument

Introduction

Oral drug administration offers obvious advantages particularly in the treatment of chronic conditions and for mass administration. However, achievement of effective drug concentrations at the disease site or therapeutic targets may be challenged by multiple interrelated physicochemical, biopharmaceutical, physiological, and clinical barriers.[1,2] In recent years, nanoformulations have emerged as prominent strategy for increasing the bioavailability and efficacy of diverse orally administered drugs and biomolecules. Most investigated systems include nanosuspensions[3] and nanoparticles

Correspondence: Alyaa A Ramadan
Department of Pharmaceutics, Faculty of Pharmacy, Alexandria University, 1 Khartoum Square, Azarita, Alexandria 21521, Egypt
Tel +20 12 2115 1295
Fax +20 3 487 3273
Email alyaa.ramadan@alexu.edu.eg

submit your manuscript | www.dovepress.com
Dovepress
http://dx.doi.org/10.2147/IJN.S167285

(NPs) of the polymer-based,[4] lipid-based,[5] and hybrid[6,7] types in addition to mesoporous silica and carbon NPs.[8,9]

Strategies to overcome intestinal barriers include the enhancement of mucus permeability by controlling NPs' size and surface charge and by decorating the NPs' surface with polyethylene oxide[10] or mucin-cleaving enzymes.[11,12] Increased oral absorption has also been achieved by inhibiting the P-gp efflux pump and utilizing the bile acid pathway.[13,14] Biomimetic drug-imprinted polymer NPs were shown to increase the efficacy of orally administered drugs.[15,16] However, targeting distal postabsorption sites implies the translocation of NPs across the intestinal epithelium. This depends, to a great extent, on the structural integrity of NPs, a further design challenge. Nevertheless, such advancements have been associated with NP-related concerns such as biodegradability, biocompatibility, cytotoxicity/genotoxicity,[17] and nanotoxicity.[18,19]

Lipid nanocapsules (LNCs), relatively new biomimetic nanocarriers,[20] appear to integrate many of the prerequisites for nanocarrier-mediated oral drug delivery. They consist of a lipid core stealth-coated nanostructure with a relatively rigid phospholipid/ethoxylated surfactant shell, prepared using a low energy phase-inversion temperature method and approved ingredients. LNCs are characterized by a size range of 20–100 nm, structural stability in simulated gastrointestinal (GI) media,[21,22] and ability to diffuse in intestinal mucus.[23] Furthermore, LNCs are taken up by Caco-2 cells via size-independent active endocytosis, a process affected by P-gp[24,25] in addition to size-dependent passive transport.[24] LNCs were shown to exhibit no genotoxicity or cytoxicity except for Kolliphor® HS 15.[26,27] The prospective use of LNCs as oral nanovectors was verified by the bioavailability and/or activity enhancement of diverse drugs including paclitaxel,[28] Sn38,[22] fondaparinux,[29] and miltefosine (MFS).[30]

Praziquantel (PZQ) is the current mainstay of schistosomiasis treatment worldwide, although with several limitations including mainly large dose (40 mg PZQ/kg),[8] poor bioavailability, and relatively short half-life due to its racemic nature and extensive first pass effect.[31] Lipid-based delivery systems, particularly solid lipid NPs,[32,33] liposomes,[34,35] and nanoemulsions[36] were shown to improve PZQ bioavailability. The objective of the present study was to gain more insight into LNCs as oral nanocarriers with potential postabsorption targeting ability using PZQ. Assessments of PZQ–LNCs as a potential single oral dose nanoformulation for the treatment of schistosomiasis mansoni were based on in vivo anti-schistosomal activity, pharmacokinetic (PK) data, scanning electron microscopy (SEM) imaging of worms recovered from mesenteric/hepatic veins of infected mice, and in vitro cytotoxicity.

Materials and methods

Materials

PZQ was obtained from Egyptian International Pharmaceuticals Industries Co (EIPICO) (Cairo, Egypt). Labrafac® lipophile WL 1349 (caprylic-capric acid triglycerides; *European Pharmacopeia*, IVth, 2002) was obtained from Gattefossé SA (Saint-Priest, France). Kolliphor HS 15 (a mixture of free polyethylene glycol 660 and polyethylene glycol 660 hydroxystearate, *European Pharmacopeia*, IVth, 2002) was obtained from BASF (Ludwigshafen, Germany). Lipoid S100 (a soybean lecithin containing 94% of phosphatidylcholine) was obtained from Lipoïd GMBH (Ludwigshafen, Germany). Oleic acid (OA) was obtained from Sigma-Aldrich Co. (St Louis, MO, USA). Miltefosine (MFS) (1-hexadecylphosphocholine) was obtained from Chem-Impex International (New York, NY, USA). HPLC grade acetonitrile was obtained from Thermo Fisher Scientific (Waltham, MA, USA). Span® 80 (sorbitan monooleate) was obtained from LobaChemie for Laboratory Reagents and Fine Chemicals (Mumbai, India). All other chemicals were of analytical grade.

Preparation of PZQ–LNCs

LNC formulations were prepared using the phase inversion method initially reported by Heurtault et al[20] with modification. In preliminary experiments, PZQ–LNCs with different compositions were prepared using Lipoid (2.8%, w/w) as lipophilic surfactant. This was replaced with Span 80 (hydrophilic lipophilic balance [HLB] 1.8) in the final formulations. In brief, PZQ was added to Labrafac (30%, w/w), Kolliphor HS 15 (25%, w/w), Span 80 (1.8%, w/w), filtered deionized water, and NaCl solution (0.88%, w/w, in deionized water). After magnetic stirring, the mixture was subjected to three progressive heating and cooling cycles between 65 and 85°C at 4°C/min. An irreversible shock was induced by twofold dilution with cold deionized water (0°C–2°C) added at 1°C–3°C from the beginning of the phase inversion zone (PIZ). This was followed by slow magnetic stirring at room temperature for 5 min. For LNC formulations modified with OA (6%, w/w) and MFS (0.2%, w/w), additives were incorporated in the emulsion mixture, which was subjected to temperature cycling between 45 and 75°C and quenching at 60°C. PZQ was added to LNC formulations at two concentration levels, 5 and 25 mg/mL of the final dispersion. The following four LNC formulations were used: PZQ–LNC-5, PZQ–LNC-25, PZQ–OA–MFS–LNC-5,

and PZQ–OA–MFS–LNC-25. LNCs were freshly prepared and used within 24 h.

In vitro characterization of PZQ–LNCs

Colloidal properties

The *z*-average particle size (PS), polydispersity index (PDI), and zeta potential (ZP) of LNCs were measured by photon correlation spectroscopy (PCS) (PCS Zetasizer® Nano ZS Series DTS 1060; Malvern Instruments, Malvern, UK). Samples were diluted 1:30 (v/v) with filtered deionized water prior to measurements.

Percent entrapment efficiency (EE%)

The EE% of PZQ–LNC formulations was determined using a dialysis technique after checking for PZQ dialyzability. PZQ–LNC dispersion (100 µL) was dialyzed through presoaked dialysis bags suspended in phosphate buffer solution (pH 7.4) for 2 h at 2°C–8°C. The free drug in dialysate was determined by HPLC–UV method as described later. The drug payload (mg/g) was calculated from the weight of PZQ entrapped in the total dry weight of LNCs.

PZQ was determined using the USP 2007 HPLC–UV method (HPLC-1260 Infinity Agilent Technologies equipped with a isocratic pump, a variable wavelength UV/Vis detector, and a manual injector) at room temperature on a reversed-phase Equisil® BDS-C18 column (250×4.6 mm, 5 µm), equipped with a 5 mm security guard column (Equisil; Maisch GmbH, Ammerbuch, Germany). An isocratic mobile phase consisting of acetonitrile and water (70:30) was injected (20 µL), and the flow rate was adjusted to 1 mL/min. PZQ was detected at λ_{max} 210 nm, and a calibration curve (0.5–25 µg/mL) for peak area ratios and a regression equation were used for PZQ determination.

In vitro release study

PZQ release from PZQ–LNC dispersions was assessed in phosphate buffered saline (PBS) (pH 7.4) containing 0.002% Tween 80 using a dialysis method in a thermostatically controlled shaking water bath (100 strokes/min) at 37°C±0.5°C (PZQ solubility under the release conditions was 70±2 µg/mL). PZQ suspension 25 mg/mL was used as control. At fixed time intervals, 1 mL samples were withdrawn and replaced with an equal volume of fresh medium at 37°C±0.5°C. PZQ was assayed as described.

Antischistosomal activity of PZQ–LNCs in *Schistosoma mansoni*-infected mice

The study was conducted at the *Schistosoma mansoni* Biological Supply Program Unit of Theodor Bilharz Research Institute (SBSP/TBRI, Giza, Egypt) in strict accordance with the TBRI Guidelines for Ethical Conduct in Use of Animals in Research. Albino mice, aged 6–8 weeks and weighing 18–20 g, were maintained in conditioned rooms at 21°C on sterile water ad libitum and a balanced dry food containing 14% protein. Mice were infected by subcutaneous injection of 0.2 mL aliquots of a cercarial suspension containing 80 cercariae into the loose skin of the back of the mouse.[37] Mice were then kept for 42 days allowing cercariae to mature into adult worms. Mice were then randomly divided into four groups, six mice each. Mice in the treatment groups were administered a single 250 mg/kg oral dose of PZQ either as an aqueous suspension in 0.002% Tween 80 or LNCs dispersion by gastric gavage. Seven days post-treatment, on the 49th day postinfection (pi), mice of all groups were sacrificed by cervical dislocation following a heparin injection.

Antischistosomal activity

This was assessed in terms of the percentage of reduction in total adult worm burden, histopathological changes in liver parenchyma, the number and size of liver granulomas, and the morphology of worms recovered from mesenteric/hepatic veins, by SEM (JFC-1100E; JEOL, Tokyo, Japan).

The percentage of reduction in total worm burden was calculated based on the number of recovered adult worms in all groups, by the perfusion technique,[38] as follows:

$$\%\ \text{reduction} = \frac{\text{Mean value (control group)} - \text{Mean value (treated group)}}{\text{Mean value (control group)}} \times 100$$

For histopathological changes in liver parenchyma, specimens of the liver of mice of all groups were fixed in 10% neutral buffered formalin. Histological sections, 5 µm thick, were stained with hematoxylin and eosin, and hepatic parenchyma was examined by light microscopy. The number of granulomas in 10 successive fields in at least five slides from each mouse was examined. The mean value of 10 readings for each mouse was calculated, and the mean number of granulomas was calculated for each group. The diameters of granulomas were measured under a light microscope equipped with an ocular micrometer. Only granulomas containing one clearly identifiable, central egg were selected. For each mouse, the mean diameter of 10 granulomas was determined and the mean size of granulomas estimated for each group.

For SEM imaging, adult worms were collected from the hepatic and mesenteric veins of mice of all groups 24 h after drug administration. Worms were fixed in 2.5% glutaraldehyde in phosphate buffer (pH 7.4) and sputter coated with an ultrathin gold coat for SEM imaging.

PK study

The PK study was conducted in accordance with the guidelines adopted by the Institutional Animal Care and Ethical Committee of the Faculty of Pharmacy, Alexandria University, which also approved the experimental procedure (approval no ACUC/32). Fifteen female Wistar rats (200–260 g) were divided into three equal groups and fasted overnight prior to the experiment. A single 250 mg/kg oral dose of PZQ as PZQ–LNC-25 and PZQ–OA–MFS–LNC-25 test formulations was administered by gastric gavage using an aqueous PZQ suspension (25 mg/mL) as control. Blood samples were collected via the orbital plexus under anesthesia at prescheduled time intervals for 4 h for PZQ suspension and 24 h for PZQ–LNCs. Blood samples were centrifuged at 4,000 rpm for 10 min, and plasma samples were immediately frozen at −20°C pending analysis.

Aliquots of rat plasma, 300 µL each, were vortex-mixed with 900 µL acetonitrile for 1 min and centrifuged at 14,000 rpm for 10 min. The organic phase was transferred to a clean tube and evaporated under nitrogen. This was followed by lyophilization and reconstitution of the residue in 100 µL of acetonitrile. PZQ in plasma was determined by the HPLC–UV method as described earlier. The method was validated for plasma samples and PZQ quantification achieved using calibration graphs for peak areas of PZQ in spiked plasma (0.1–10 µg/mL) obtained under similar conditions. Plasma concentrations versus time data were analyzed noncompartmentally using the Excel PK solver add-in.

Stability in simulated GI fluids

The stability of freshly prepared PZQ–LNCs in simulated gastrointestinal (GIT) fluids (USP 33-28NF2010) was examined, as reported.[21] Briefly, simulated gastric fluid (SGF) (pH 1.2) (2 g of NaCl and 3.2 g of pepsin in 7 mL HCl and the volume made up to 1,000 mL) and simulated intestinal fluid (SIF) (pH 6.8) (6.8 g of KH_2PO_4 in 250 mL water to which was added 77 mL of 0.2 N NaOH, 500 mL of water, and 10 g of pancreatin). LNC dispersions were diluted to a final concentration of 10% (v/v) in simulated GI fluids and incubated at 37°C. Samples were withdrawn at 0, 1, 2, and 3 h. An additional 6 h sample was withdrawn for SIF. The size of collected LNCs was measured by PCS, and the EE% calculated by HPLC after the separation of LNCs by centrifugation for 30 min at 3,663× *g* using ultracentrifugal concentrators (MWCO 100,000, Vivaspin6™; Sartorius, Göttingen, Germany).

In vitro cytotoxicity study

Human peripheral blood mononuclear cells (PBMCs) were used to assess the in vitro cytotoxicity of LNCs in comparison with PZQ solution in ethanol. PBMCs were obtained from a 20 mL blood sample donated by a healthy volunteer under medical supervision. The procedure was approved by the Research Ethics Committee of the Faculty of Pharmacy, Alexandria University, after obtaining the written informed consent of the volunteer (approval no 1762). LNC samples, sterilized using 0.22 µm sterile syringe filters, were serially diluted in a 96-well plate for different PZQ concentrations (0.3–100 µg/mL). Cell suspension at 1×10^6 cells/mL was added to dispersions of the test formulations (100 µL/well). Control wells were prepared by adding 100 µL of culture medium to the cell suspension. The plate was incubated at 37°C, 5% CO_2 for 24 h, and the cell viability was assessed using the 3-(4,5-dimethiazol-zyl)-2-5-diphenyltetrazolium bromide (MTT) assay at 570 nm[39] in triplicate. Dose–response curves were plotted, and IC_{50} values were calculated.

Statistical analyses

Antischistosomal activity data were analyzed using the IBM SPSS software Version 20.0. Kolmogorov–Smirnov test was used to verify the normality of variables' distribution. Quantitative data were described using range, mean, standard deviation, and median. For normal quantitative variables, *F*-test (analysis of variance [ANOVA]) was used to compare more than two groups and post hoc test (Tukey) was used for pair-wise comparisons. For abnormal quantitative variables, Mann–Whitney test was used to compare two groups and Kruskal–Wallis test was used to compare more than two groups. Other results were analyzed using the paired *t*-test. *P*-values ≤0.05 indicated statistical significance.

Results

Formulation of PZQ–LNCs

Based on a series of preliminary experiments using Labrafac, Kolliphor, and either Lipoid or Span 80, a PZQ-LNC formulation with the basic composition, Labrafac (30%, w/w), Kolliphor HS 15 (25%, w/w), and Span 80 (2%, w/w), was selected. Span 80 reduced the phase inversion temperature (PIT) to 68°C. LNC composition was further modified by the inclusion of OA (6%, w/w), resulting in a lower heating/cooling temperature range (45°C–65°C).[32] MFS was also

Table 1 Physicochemical properties of blank and PZQ-loaded LNC formulations (n=3)

Code	PZQ (mg/mL)	Mean size (nm)	PDI	ZP (mV)	EE%	Payload (mg/g)
LNC	–	57.8±1.1	0.04	−5.8±1.4	–	–
PZQ–LNC-5	5	54.7±2.5	0.08	−3.8±0.7	95.7±0.5	17.5
PZQ–LNC-25	25	61.8±2.7	0.04	−7.5±1.8	95.1±0.8	84.9
OA–MFS–LNC	–	52.9±1.13	0.01	−7.6±0.5	–	–
PZQ–OA–MFS–LNC-5	5	46.8±1.2	0.03	−4.2±1.7	97.0±0.9	17.6
PZQ–OA–MFS–LNC-25	25	50.8±0.1	0.04	−8.9±2.3	99.8±0.1	86.3

Abbreviations: EE%, entrapment efficiency; LNC, lipid nanocapsules; MFS, miltefosine; OA, oleic acid; PDI, polydispersity index; PZQ, praziquantel; ZP, zeta potential.

added to the LNCs (0.2%, w/w) without further effects either on PIT or on temperature range.

Characteristics of PZQ–LNCs

The physicochemical properties of LNC formulations are shown in Table 1. Blank LNCs had a mean diameter of 57.8 nm and were generally uniform (PDI 0.04) with a ZP of −5.8 mV. Loading LNCs with PZQ or modifying their composition with OA and MFS slightly but significantly ($P<0.05$) affected their colloidal properties. EE% values generally exceeded 95%. Increasing the initial PZQ concentration from 5 to 25 mg/mL of LNC dispersion resulted in a significant increase in drug payload (Table 1).

In vitro PZQ release in PBS (pH 7.4)/0.002% Tween 80 at 37°C under sink conditions showed almost complete release of free PZQ in 1 h, indicating dialyzability (Figure 1). LNC formulations showed biphasic release profiles with a relatively small burst effect (12.6%–19.0% in 30 min), indicating efficient drug entrapment, yet a greater burst effect was observed at higher initial drug loading. The difference was statistically significant for PZQ–LNCs ($P<0.05$). The extent of PZQ release from LNCs in 24 h ranged from 44.6% to 48.4%.

Antischistosomal activity in *S. mansoni*-infected mice

Encapsulation of PZQ in LNCs resulted in a significant increase in antischistosomal activity upon administration of a single 250 mg/kg oral dose of LNCs, compared to PZQ suspension to *S. mansoni*-infected mice. Efficacy assessment was based on changes in worm burden count, the size and number of granuloma, and the histopathology of liver sections.

Data for worm burden and their statistical analysis are shown in Table 2. Untreated mice showed a mean total worm load of 24.67±1.86, which was significantly reduced by PZQ suspension (70.9%). The two PZQ–LNC formulations exerted a significantly greater reduction in worm

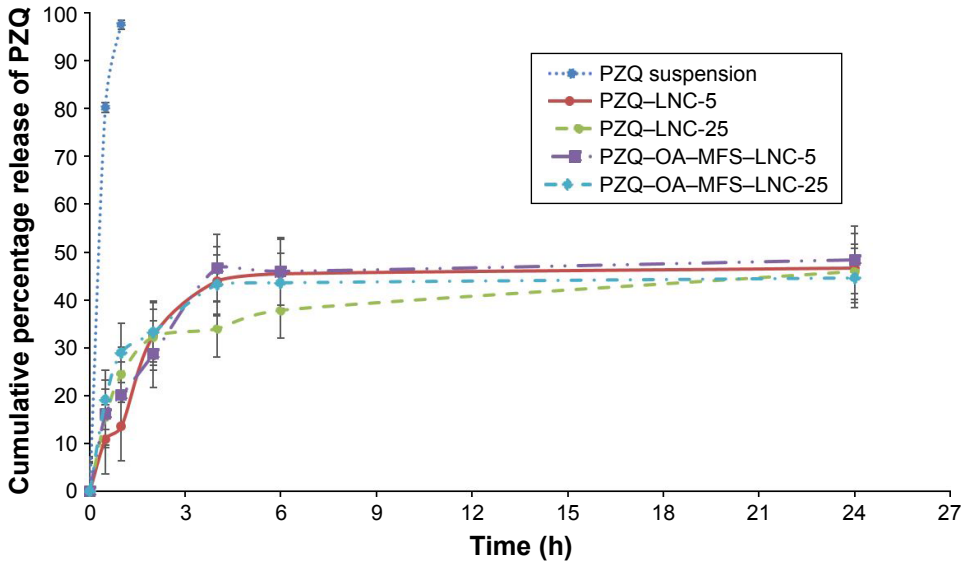

Figure 1 Release of PZQ from PZQ–LNC and PZQ–OA–MFS–LNC formulations containing 5 or 25 mg/mL of PZQ in comparison to PZQ in PBS (pH 7.4) at 37°C.
Note: Data represent mean ± SD (n=3).
Abbreviations: LNC, lipid nanocapsules; MFS, miltefosine; OA, oleic acid; PZQ, praziquantel.

Table 2 Effect of single 250 mg/kg oral dose of PZQ–LNC formulations in comparison with PZQ suspension on the total worm load recovered from *S. mansoni*-infected mice and reduction in adult worm burden (n=5)

Worm load	Animal group/formulation code				Significance test
	Group 1: untreated control	Group 2: PZQ suspension	Group 3: PZQ–LNC-25	Group 4: PZQ–OA–MFS–LNC-25	
Total worm load					
Minimum	22.0	6.0–8.0	0.0–3.0	0.0–3.0	*H*=20.066* *P*<0.001*
Maximum	27.0	6.0–8.0	0.0–3.0	0.0–3.0	
Mean	24.67	7.17	1.83	2.0	
SD	1.86	0.98	0.98	1.10	
Median	25.0	7.50	2.0	2.0	
Percentage of reduction		70.9	92.6	91.9	
P-value	*P*1=0.004*, *P*2=0.003*, *P*3=0.004*, *P*4=0.003*, *P*5=0.003*, *P*6=0.652				

Notes: Percentage of reduction: percentage of reduction between each group and Group 1. *H*: Kruskal–Wallis test, significance between groups was done using Mann–Whitney test. *P*1: *P*-value for comparison between Groups 1 and 2. *P*2: *P*-value for comparison between Groups 1 and 3. *P*3: *P*-value for comparison between Groups 1 and 4. *P*4: *P*-value for comparison between Groups 2 and 3. *P*5: *P*-value for comparison between Groups 2 and 4. *P*6: *P*-value for comparison between Groups 3 and 4. *Statistically significant at $P \leq 0.05$.

Abbreviations: LNC, lipid nanocapsule; MFS, miltefosine; OA, oleic acid; PZQ, praziquantel; *S. mansoni*, *Schistosoma mansoni*.

load (92.6 and 91.9% for PZQ–LNC-25 and PZQ–OA–MFS–LNC-25, respectively) compared to PZQ suspension. A similar pattern was observed for the reduction in the number and size of granuloma (Table 3), though the reduction induced by the two PZQ–LNC formulations was not statistically significant.

Histopathological changes in liver sections of infected untreated mice are shown in Figure 2A–E. Preserved hepatic architecture with multiple portal and parenchymal granulomas of variable sizes and shapes is clear in Figure 2A. Irregularly outlined and cellular granulomas composed of lymphocytes, histiocytes, epitheliod cells, and esoinophils surrounding

Table 3 Number/LPF and size (μm) of hepatic granulomas in *S. mansoni*-infected mice in the different study groups (n=5)

Parameter	Treatment				*F* (P)
	Group 1: control	Group 2: PZQ suspension	Group 3: PZQ–LNC-25	Group 4: PZQ–OA–MFS–LNC-25	
Number of granuloma/LPF					308.931* (<0.001*)
Minimum	29.0	18.0	10.0	11.0	
Maximum	32.0	21.0	14.0	14.0	
Mean	30.7	19.3	12.2	12.7	
SD	1.1	1.0	1.5	1.0	
Median	30.5	19.0	12.5	13.0	
Percentage of reduction		↓37.0	↓60.3	↓58.7	
P-value	*P*1<0.001*, *P*2<0.001*, *P*3<0.001*, *P*4<0.001*, *P*5<0.001*, *P*6=0.887				
Diameter of granuloma (μm)					54.204* (<0.001*)
Minimum	400	257	165	173	
Maximum	4,710	377	268	306	
Mean	437	296	200	217	
SD	26	41	40	49	
Median	437	283	189	189	
Percentage of reduction		↓32.2	↓54.1	↓50.4	
P-value	*P*1<0.001*, *P*2<0.001*, *P*3<0.001*, *P*4<0.001*, *P*5=0.003*, *P*6=0.852				

Notes: Percentage of reduction: percentage of reduction between each group and Group 1. *F*: *F* value for ANOVA test, significance between groups was done using post hoc test (Tukey). *P*1: *P*-value for comparison between Groups 1 and 2. *P*2: *P*-value for comparison between Groups 1 and 3. *P*3: *P*-value for comparison between Groups 1 and 4. *P*4: *P*-value for comparison between Groups 2 and 3. *P*5: *P*-value for comparison between Groups 2 and 4. *P*6: *P*-value for comparison between Groups 3 and 4. *Statistically significant at $P \leq 0.05$.

Abbreviations: ANOVA, analysis of variance; LNC, lipid nanocapsules; LPF, low power field; MFS, miltefosine; OA, oleic acid; PZQ, praziquantel; *S. mansoni*, *Schistosoma mansoni*.

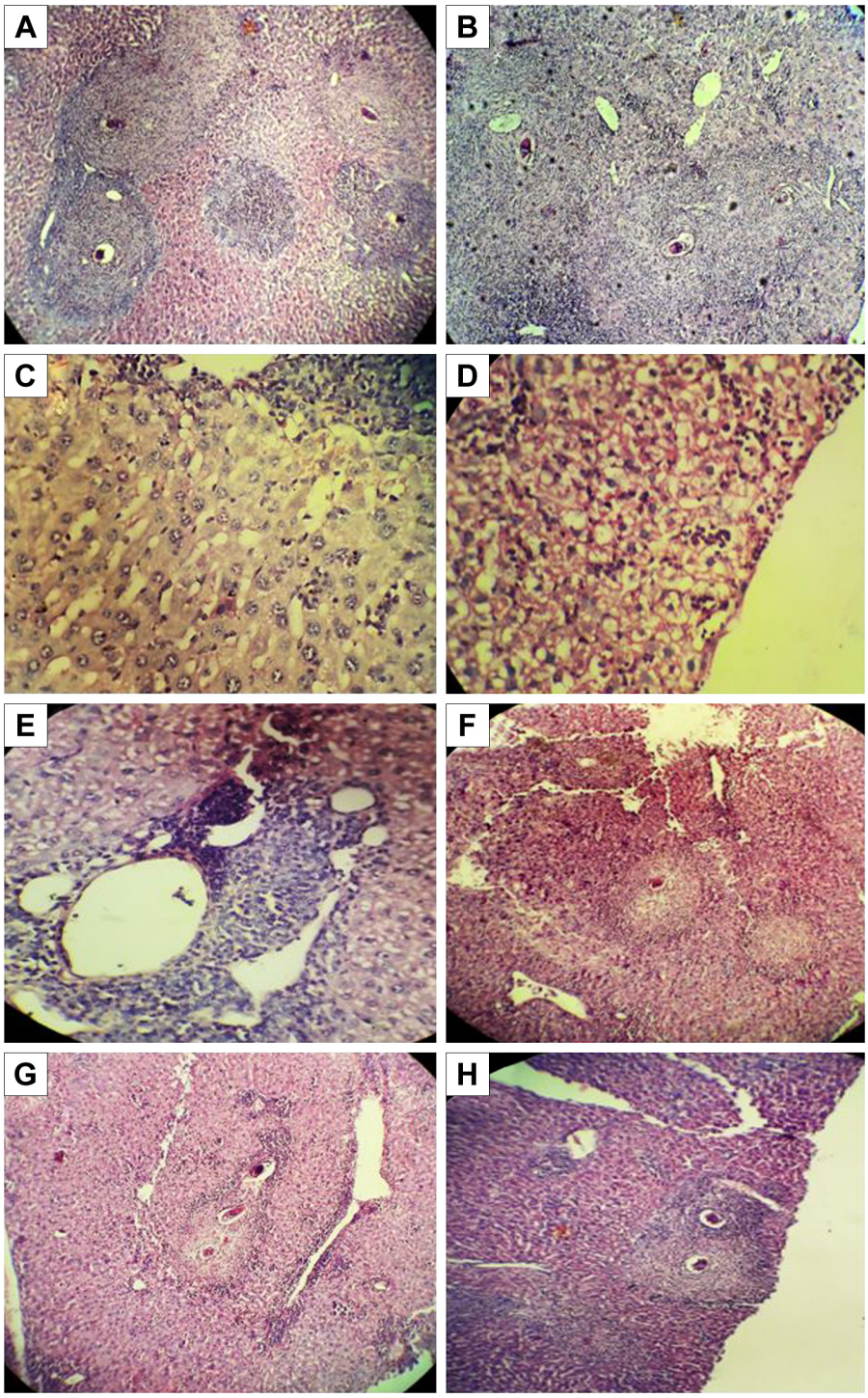

Figure 2 Histopathological study of H&E-stained liver sections of different groups of mice infected with *Schistosoma mansoni*.
Notes: Infected untreated group showing: (**A**) multiple granulomas of variable sizes and shapes with preserved hepatic architecture (×100); (**B**) cellular granuloma composed of lymphocytes, histiocytes, epithelioid cells, and eosinophil cells, surrounding the bilharzial egg (×400); (**C**) Kupffer cell hyperplasia and bilharzial pigment (×400); (**D**) fatty changes in hepatocytes (×400); (**E**) hepatic sinusoids with lymphocytic infiltration (×400); and (**F**) infected PZQ suspension-treated mice (×100); (**G**) infected PZQ–LNC-25-treated mice (×100), and (**H**) infected PZQ–OA–MFS–LNC-25-treated mice (×100) showing small cellular granulomas with mild amelioration of liver pathology.
Abbreviations: LNC, lipid nanocapsules; MFS, miltefosine; OA, oleic acid; PZQ, praziquantel.

recently deposited intact or partially degenerated eggs could be observed in Figure 2B. Hyperplasia of Kupffer cells, deposition of bilharzia pigment (Figure 2C), and fatty changes in hepatocytes (Figure 2D) were also observed. The hepatic sinusoids showed lymphocytic infiltration (Figure 2E). Liver sections of PZQ suspension and PZQ–LNC-treated mice showed scanty small hepatic granulomas with amelioration of hepatic pathology (Figure 2F). However, marked improvement

was more evident in liver sections of mice treated with the two LNC formulations (Figure 2G and H).

SEM images of male worms recovered from the hepatic and mesenteric veins of mice of all groups are shown in Figure 3. Worms from untreated mice (Group 1) showed round to oval oral and ventral suckers (Group 1A). The dorsolateral surface of the mid-body was covered with well-developed tubercles of uniform size and distribution (Group 1B), and the intact tegument surface showed apically directed spines (Group 1C). Worms from the PZQ suspension-treated group (Group 2) showed distorted oral suckers (Group 2A), tegumental damage in the form of surface erosion with the flattening of some tubercles (Group 2B), and distorted spines (Group 2C). Worms from PZQ–LNC-25-treated mice (Group 3) showed more distorted oral suckers (Group 3A), severe tegumental damage manifested as damaged tubercles and eroded tegument with the appearance of sub-tegumental tissue (Group 3B), and severely distorted spines (Group 3C). Similar extensive damage to the worm tegument and spines was observed in PZQ–OA–MFS–LNC-25-treated mice (Group 4A–C).

PK study

The plasma concentration versus time profiles for PZQ–LNC-25 and PZQ–OA–MFS–LNC-25 in comparison with PZQ suspension following administration of a single 250 mg/kg oral dose to female Wistar rats are shown in Figure 4. Validation data for the HPLC–UV method used for PZQ quantitation in plasma indicated linearity over the concentration range of 0.1–100 µg/mL (R^2=0.9998), the limit of detection (LOD) and limit of quantification (LOQ) values of 3.142 and 9.55 µg/mL, respectively, and a coefficient of variation for intra-day and inter-day precisions for three quality control PZQ solutions (7, 3, and 1 µg/mL) <7.8%.

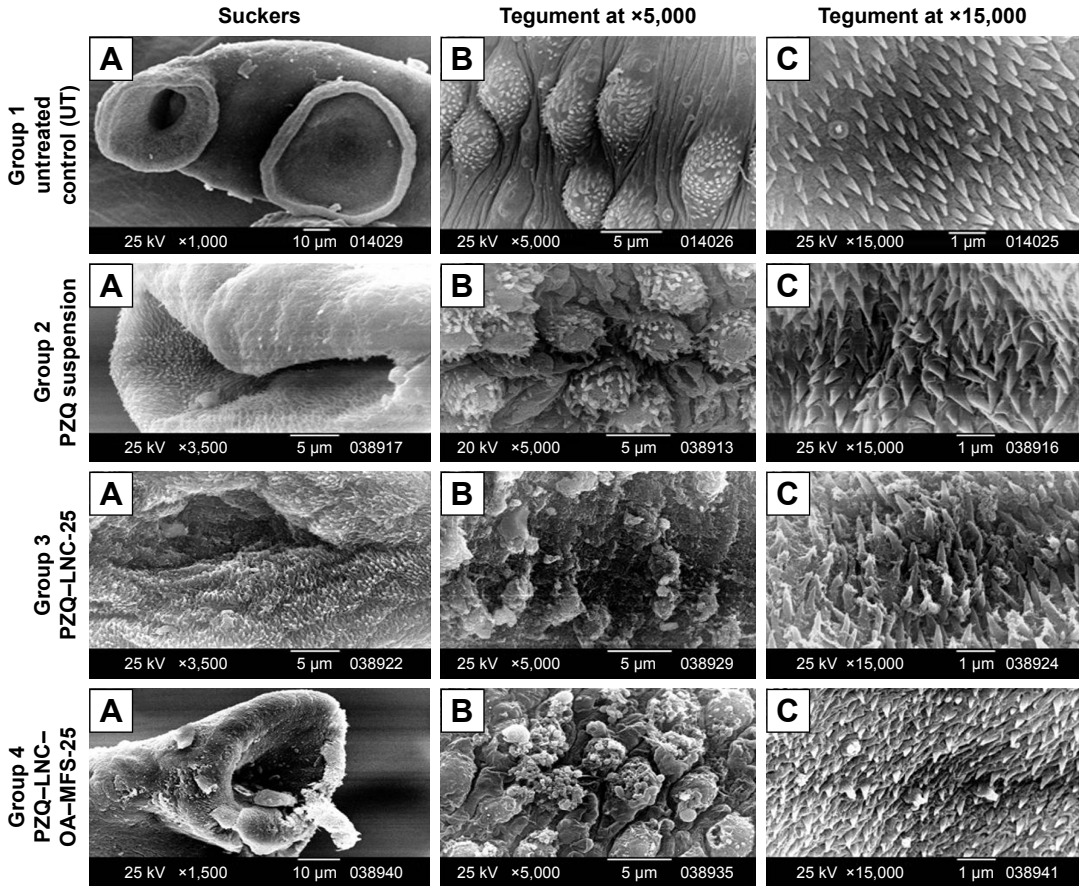

Figure 3 SEM images of male worms recovered from the hepatic and mesenteric veins of mice of the four study groups.

Notes: SEM of a male *Schistosoma mansoni* worm recovered from infected untreated mice (Group 1) showing (**A**) normal OS and VS (×1,000), (**B**) dorsal tegument surface with uniform size, regularly distributed T, and visible S (×5,000), and (**C**) apically situated S (×15,000); infected PZQ suspension-treated mice (Group 2) showing (**A**) distorted OS (×3,500), (**B**) flattening of some T with loss of S (×5,000), and (**C**) distorted S (×15,000); infected PZQ–LNC-25-treated mice (Group 3) showing (**A**) distorted OS (×3,500), (**B**) severe tegumental damage with erosion of the surface and appearance of subtegumental tissue (×5,000), and (**C**) distorted S (×15,000); and infected PZQ–OA–MFS–LNC-25-treated mice (Group 4) showing (**A**) distorted OS (×1,500), (**B**) severe tegumental damage with erosion of the surface and appearance of subtegumental tissue (×5,000), and (**C**) distorted S (×15,000).

Abbreviations: LNC, lipid nanocapsules; MFS, miltefosine; OA, oleic acid; OS, oral sucker; PZQ, praziquantel; S, spines; SEM, scanning electron microscopy; T, tubercles; VS, ventral sucker.

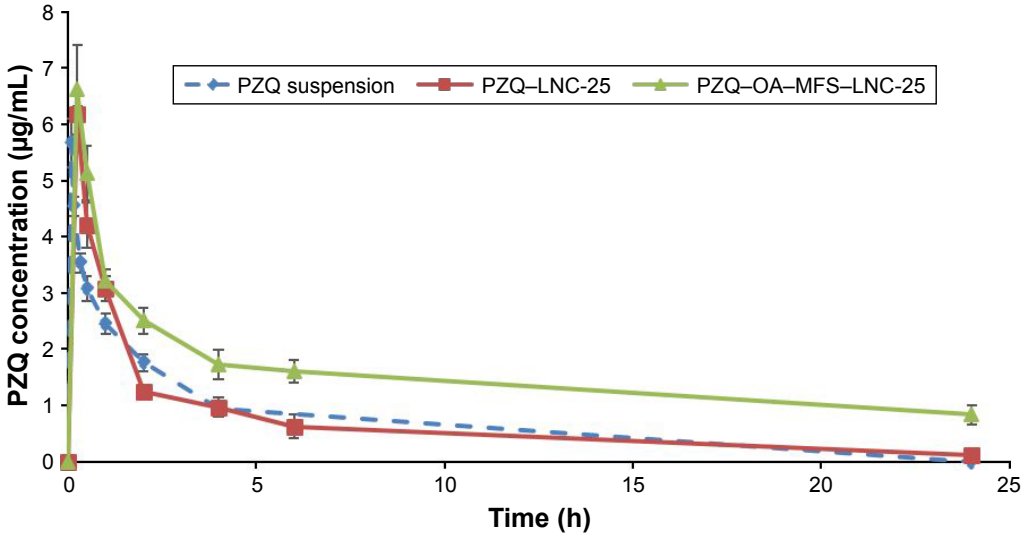

Figure 4 Mean plasma levels of PZQ following oral administration of 250 mg/kg dose of PZQ as suspension and LNC formulations to rats (n=5).
Note: Error bars represent standard error of the mean.
Abbreviations: LNC, lipid nanocapsules; MFS, miltefosine; OA, oleic acid; PZQ, praziquantel.

The PK parameters calculated by noncompartmental analysis are listed in Table 4. Peak plasma concentration for PZQ suspension (5.5±1.9 µg/mL) was reached after 6±2.4 min. A significant increase in time to reach maximum plasma concentration (t_{max}) was observed for PZQ–LNCs (20±7.8 and 22±8.4 min for PZQ–LNC-25 and PZQ–OA–MFS–LNC-25, respectively). Although a slight increase in maximum plasma concentration (C_{max}) was observed for PZQ–LNC formulations compared to PZQ suspension, the difference did not reach statistical significance. In contrast, a significant increase in AUC_{0-inf} ($P<0.05$) was observed. This was in line with the significant increase in half-life ($t_{1/2}$) and mean residence time (MRT) ($P<0.05$). Statistical analysis indicated that differences in PK parameters of the two PZQ–LNC formulations were not significant (Table 4).

Table 4 Pharmacokinetic parameters of PZQ after a single oral dose (250 mg/kg) of PZQ suspension or PZQ–LNC formulations (n=5)

Pharmacokinetic parameter	PZQ suspension	PZQ–LNC-25	PZQ–OA–MFS–LNC-25
$t_{1/2}$ (h)	1.7±0.8	5.7±1.0	8.9±2.9
t_{max} (min)	6.0±2.4	20±7.8	22.0±8.4
C_{max} (µg/mL)	5.5±1.9	6.2±0.5	6.5±3.1
AUC_{0-t} (µg/mL h)	7.9±2.2	14.8±5.7	19.0±5.9
AUC_{0-inf_obs} (µg/mL h)	9.9±1.5	18.9±4.3	27.2±7.5
MRT_{0-inf_obs} (h)	3.4±2.0	7.6±2.8	12.7±4.1

Abbreviations: LNC, lipid nanocapsules; MFS, miltefosine; OA, oleic acid; PZQ, praziquantel; $t_{1/2}$, plasma, half-life; t_{max}, time to reach maximum plasma concentration; C_{max}, maximum plasma concentration; AUC, area under the curve; MRT, mean residence time.

GI stability

The particle size (PS) of both PZQ–LNC-25 and PZQ–OA–MFS–LNC-25 did not significantly change after 3 h incubation in SGF. However, a limited (<10%), though significant decrease in EE%, was observed over 3 h. Both formulations retained their size for the first hour in SIF containing 1% (w/v) pancreatin at pH 6.8. This was followed by aggregation. EE% data indicated no PZQ leakage over the 6 h incubation.

In vitro cytotoxicity study

Cytotoxicity data obtained for PZQ–LNC-25 and PZQ–OA–MFS–LNC-25 in comparison with blank LNCs and PZQ solution in ethanol in PBMCs are shown in Figure 5. Blank LNCs showed in vitro cytotoxicity (IC_{50} 63.4 µg/mL), which was significantly increased by the incorporation of OA and MFS (IC_{50} 43.4±1.1 µg/mL). Furthermore, loading LNCs with PZQ did not change the cytotoxicity of the corresponding blank LNCs considerably, under the study conditions. IC_{50} values for PZQ–LNCs (58.9±5.3 and 43.4±1.1 µg/mL for PZQ–LNC-25 and PZQ–OA–MFS–LNC-25, respectively) were larger than that of free PZQ (IC_{50} 11.0±2.2 µg/mL).

Discussion

LNCs exhibit unique properties, particularly small size range and structural stability, favoring their use as oral nanocarriers.[20,30] In the present study, their potential for oral targeting ability was assessed using PZQ, a large dose antischistosomal drug. The current mainstay strategy for schistosomiasis chemotherapy involves mass administration

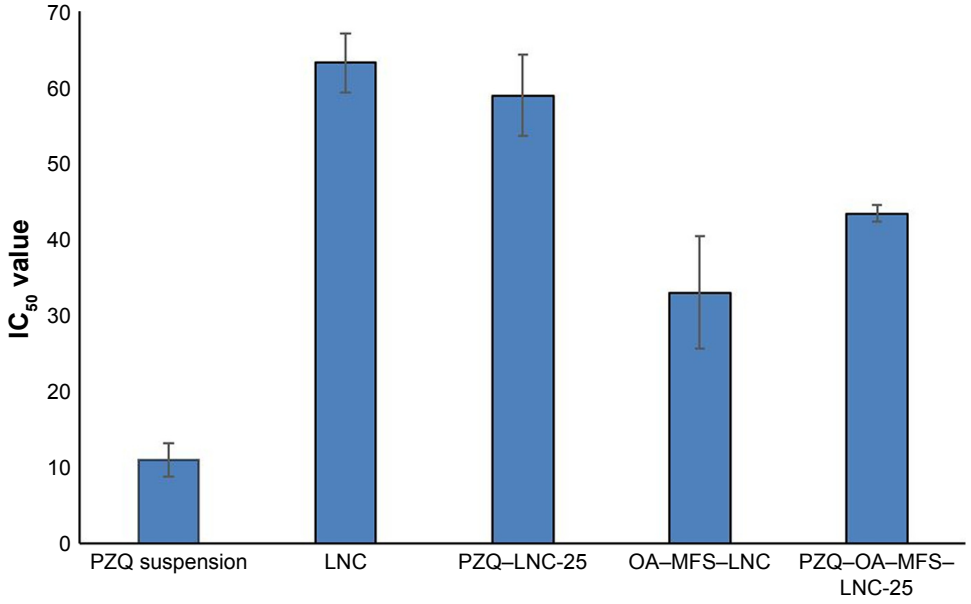

Figure 5 Cytotoxic effect of PZQ-loaded LNCs in comparison to PZQ solution on PBMCs using MTT assay and expressed as IC_{50} values after 24 h of incubation.
Abbreviations: LNCs, lipid nanocapsules; MFS, miltefosine; MTT, 3-(4,5-dimethiazol-zyl)-2-5-diphenyltetrazolium bromide; OA, oleic acid; PBMCs, peripheral blood mononuclear cells; PZQ, praziquantel.

of a single oral dose of PZQ.[40] Thus, PZQ–LNCs with a relatively high drug loading, small size, and enhanced membrane permeability were formulated.

In a preliminary trial, PZQ–LNCs were prepared using Lipoid as a structure-enforcing lipophilic phospholipid surfactant, which, in conjunction with the hydrophilic surfactant Kolliphor, acts as emulsion stabilizer during LNC formation.[20] Results obtained using LNC formulations that included Labrafac (19%–30%, w/w), Kolliphor (19%–25%, w/w), and Lipoid (2.8%, w/w) indicated PZQ incorporation up to 15 mg/mL of LNC dispersion. This might not allow a curative PZQ dose in preclinical testing. The PZQ dose in mice ranges from 400 to 1,350 mg/kg.[41] Substituting Span 80 2% (w/w) for Lipoid allowed increase of PZQ concentration to 25 mg/mL. The reduction in PIT observed for Span 80 formulations can be attributed to a reduction in the oil/aqueous phase interfacial tension.[42]

Furthermore, OA was added to modify the fluidity of LNCs and permeabilize cell membrane for enhanced LNC-cell interaction and intestinal transport.[43,44] The reduction in heating–cooling range during LNC formation could be explained by OA-induced fluidization of the surfactant monolayer[45] and partial incorporation of some OA molecules into the surfactant film of the microemulsion phase.[46] MFS was incorporated for enhancing LNC structural integrity and imparting membrane activity.[30] Inclusion of both additives resulted in slight changes in colloidal properties of PZQ–LNCs (Table 1), indicating uniform PZQ distribution within the LNC core, the reduction in size being attributed to enhanced emulsification during LNCs' formation.[30] Similar to other lipophilic drugs such as paclitaxel and albendazole,[28,47] PZQ was efficiently entrapped in the LNCs oily core (EE >95%) allowing a payload of 86.3 mg/g for PZQ–OA–MFS–LNC-25 (Table 1).

Sustained release of PZQ (Figure 1) combined with published release data for other drugs[22,30] suggested structural integrity of LNCs, a factor of great importance to their in vivo performance. Increasing initial drug loading was associated with a greater burst effect. The difference was statistically significant only for PZQ–LNCs and not for PZQ–OA–MFS–LNCs, pointing to more effective drug entrapment by the inclusion of additives. OA was reported to increase PZQ solubility via ionic interactions and hydrogen bonding.[48]

The prepared PZQ–LNCs with low (5 mg/mL) and high (25 mg/mL) drug loading could be potential formulations for clinical applications involving relatively low or high curative PZQ doses such as in pediatric and adult oral nanomedicines, respectively. In the present study, LNCs with higher drug payload (PZQ–LNC-25 and PZQ–OA–MFS–LNC-25) were selected for pharmacodynamic (PD), PK, and cytotoxicity assessments.

The superior antischistosomal activity of both PZQ–LNC formulations in *S. mansoni*-infected mice following administration of a single oral dose of PZQ (250 mg/kg) compared to PZQ suspension (Tables 2 and 3) was substantiated by the greater damage to suckers and tegument of adult worms

(Figure 3). In fact, sucker deformity reduces the fluke's ability to adhere to blood vessels, rendering the ingestion of nutrients more difficult.[49] Tegumental damage along the worm body impairs the functioning of the tegument and destroys the worm defense system, facilitating attack by the host's immune system.[49] Combined data provided evidence for the significant enhancement of PZQ activity by LNCs formulated to possess the required attributes.

LNCs showed great promise in recent years as nanovectors for antiparasitic agents.[30,47,50,51] For instance, we demonstrated earlier that LNCs significantly enhanced the PD activity of MFS as a potential repurposed antischistosomal agent.[30,50] Efficacy of MFS–LNCs against both mature and prepatent *S. mansoni* worms in *S. mansoni*-infected mice in a single oral 20 mg/kg dose was mainly attributed to facilitation of intestinal transport and interaction with the tegument surface, an effect significantly augmented by inclusion of OA as gut membrane permeabilizer[52] and/or fusogenic agent.[43] More recently, MFS was shown to unmask parasite surface antigens not normally exposed to the host during infection, enhancing their serological recognition.[53] In the present study, inclusion of MFS and OA in PZQ–OA–MFS–LNCs did not significantly enhance antischistosomal activity (Tables 2 and 3), probably because of the lower MFS dose used (10 mg/kg) and masking of OA effects by Span 80 (sorbitan monoleate), reported to exert a fusogenic effect on phospholipid vesicles.[54]

PK data indicated an increased PZQ bioavailability (Table 4), contributing to an enhanced PD activity by LNCs. However, this may not solely depend on the increase in systemic concentration of the drug. It has been reported recently that changes in the systemic exposure to PZQ induced by an irreversible pan-cytochrome P450 (CYP) inhibitor or a CYP inducer were not predictive of efficacy in the *S. mansoni* mouse model.[55] Furthermore, validity of classical drug PK/PD relationships following oral drug administration may not entirely apply to oral nanomedicines.[23] Targeting distant sites postabsorption may greatly contribute to efficacy enhancement by nanoformulations, provided that structural integrity is maintained.[30,56,57] In the present study, stability of PZQ–LNCs in GI media, attributed to steric stabilization provided by the nonionic Kolliphor shell,[21,58] corroborated LNCs' ability to permeate through mucus[23,59] and the intestinal barrier via active endocytosis.[22,24,25] Furthermore, SEM visualization of nano-objects on the surface of the tegument of adult *S. mansoni* worms recovered from the hepatic/mesenteric veins postoral administration to infected mice (Figure 6) provided further evidence for oral targeting by LNCs, as observed earlier for MFS–LNCs.[30] It has been demonstrated that the availability of PZQ in high concentrations before the hepatic first pass metabolism is a key factor in the efficacy of PZQ against *S. mansoni* adult worms in the mesenteric veins.[55] The study outcomes combined with literature data suggest intestinal transport of more or less structurally intact PZQ–LNCs and targeting *S. mansoni* tegument as a main factor contributing to antischistosomal efficacy enhancement. From an application standpoint, PZQ–LNCs could be suggested as an oral nanotherapeutic with potential *S. mansoni* tegumental targeting.

Safety assessment of these formulations indicated that standard blank LNC formulations showed some degree of cytotoxicity to PBMCs under the study conditions, attributed to the surfactant Kolliphor.[26] Increased cytotoxicity of OA and MFS-containing LNCs can be attributed to cytotoxic effects reported on different cell lines.[60–62] PZQ–LNCs showed similar cytotoxicity to the corresponding blank formulations, supporting data for PZQ thermosensitive nanoemulsion.[36] Importantly, PZQ–LNC formulations showed better tolerability compared to free PZQ, an observation reported for PZQ solid lipid NPs.[63]

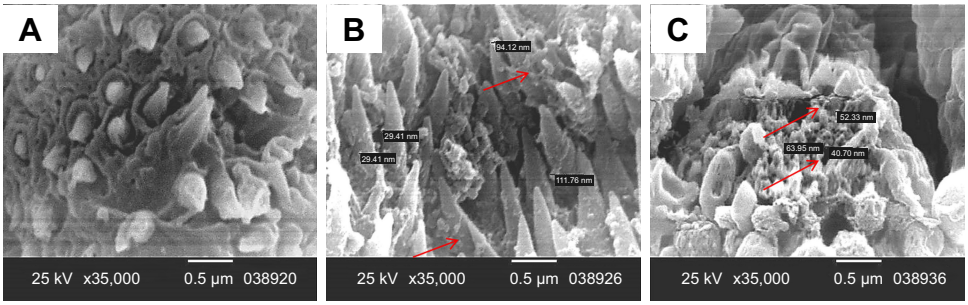

Figure 6 SEM of a male *Schistosoma mansoni* worm (×35,000) recovered from a mouse treated with (**A**) PZQ suspension, (**B**) PZQ–LNC-25 or (**C**) PZQ–OA–MFS–LNC-25 showing nanostructures of similar size to LNCs in between spines and on damaged schistosomal surface (indicated by arrows), only in worms recovered from mice treated with PZQ–LNC formulations (**B** and **C**).
Abbreviations: LNCs, lipid nanocapsules; MFS, miltefosine; OA, oleic acid; PZQ, praziquantel; SEM, scanning electron microscopy.

Conclusion

LNCs with modified composition proved highly effective as oral nanovectors for a large dose drug, PZQ. A single 250 mg/kg oral dose of PZQ–LNCs significantly enhanced PZQ antischistosomal activity in *S. mansoni*-infected mice. PD activity combined with PK data and SEM imaging provided evidence for increased PZQ bioavailability in addition to intestinal translocation of PZQ–LNCs to target adult worms, a process promoted by the GI stability of LNCs. The study outcomes suggest LNCs as nanocarriers for improving the efficacy of orally administered drugs via systemic exposure enhancement and the oral targeting of therapeutically relevant distal sites.

Disclosure

The authors report no conflicts of interest in this work.

References

1. Date AA, Hanes J, Ensign LM. Nanoparticles for oral delivery: design, evaluation and state-of-the-art. *J Control Release*. 2016;240:504–526.
2. Yu M, Yang Y, Zhu C, Guo S, Gan Y. Advances in the transepithelial transport of nanoparticles. *Drug Discov Today*. 2016;21(7):1155–1161.
3. Li Y, Hong J, Li H, et al. Genkwanin nanosuspensions: a novel and potential antitumor drug in breast carcinoma therapy. *Drug Deliv*. 2017;24(1):1491–1500.
4. Li L, Jiang G, Yu W, et al. Preparation of chitosan-based multifunctional nanocarriers overcoming multiple barriers for oral delivery of insulin. *Mater Sci Eng C Mater Biol Appl*. 2017;70(pt 1):278–286.
5. Dudhipala N, Veerabrahma K. Improved anti-hyperlipidemic activity of rosuvastatin calcium via lipid nanoparticles: pharmacokinetic and pharmacodynamic evaluation. *Eur J Pharm Biopharm*. 2017;110:47–57.
6. Joyce P, Yasmin R, Bhatt A, Boyd BJ, Pham A, Prestidge CA. Comparison across three hybrid lipid-based drug delivery systems for improving the oral absorption of the poorly water-soluble weak base cinnarizine. *Mol Pharm*. 2017;14(11):4008–4018.
7. Grigoras AG. Polymer-lipid hybrid systems used as carriers for insulin delivery. *Nanomedicine*. 2017;13(8):2425–2437.
8. Florek J, Caillard R, Kleitz F. Evaluation of mesoporous silica nanoparticles for oral drug delivery – current status and perspective of MSNs drug carriers. *Nanoscale*. 2017;9(40):15252–15277.
9. Ran F, Lei W, Cui Y, et al. Size effect on oral absorption in polymer-functionalized mesoporous carbon nanoparticles. *J Colloid Interface Sci*. 2018;511:57–66.
10. Ren T, Wang Q, Xu Y, et al. Enhanced oral absorption and anticancer efficacy of cabazitaxel by overcoming intestinal mucus and epithelium barriers using surface polyethylene oxide (PEO) decorated positively charged polymer-lipid hybrid nanoparticles. *J Control Release*. 2017;269:423–438.
11. Menzel C, Bernkop-Schnurch A. Enzyme decorated drug carriers: targeted swords to cleave and overcome the mucus barrier. *Adv Drug Deliv Rev*. 2017;124:164–174.
12. Beloqui A, Solinís MÁ, des Rieux A, Préat V, Rodríguez-Gascón A. Dextran-protamine coated nanostructured lipid carriers as mucus-penetrating nanoparticles for lipophilic drugs. *Int J Pharm*. 2014;468(1–2):105–111.
13. Mandracchia D, Trapani A, Tripodo G, et al. In vitro evaluation of glycol chitosan based formulations as oral delivery systems for efflux pump inhibition. *Carbohydr Polym*. 2017;166:73–82.
14. Fan W, Xia D, Zhu Q, et al. Functional nanoparticles exploit the bile acid pathway to overcome multiple barriers of the intestinal epithelium for oral insulin delivery. *Biomaterials*. 2018;151:13–23.
15. Paul PK, Nopparat J, Nuanplub M, Treetong A, Suedee R. Improvement in insulin absorption into gastrointestinal epithelial cells by using molecularly imprinted polymer nanoparticles: microscopic evaluation and ultrastructure. *Int J Pharm*. 2017;530(1–2):279–290.
16. Paul PK, Treetong A, Suedee R. Biomimetic insulin-imprinted polymer nanoparticles as a potential oral drug delivery system. *Acta Pharm*. 2017;67(2):149–168.
17. Iglesias T, Lopez de Cerain A, Irache JM, et al. Evaluation of the cytotoxicity, genotoxicity and mucus permeation capacity of several surface modified poly(anhydride) nanoparticles designed for oral drug delivery. *Int J Pharm*. 2017;517(1–2):67–79.
18. Patel P, Shah J. Safety and toxicological considerations of nanomedicines: the future directions. *Curr Clin Pharmacol*. 2017;12(2):73–82.
19. Saifi MA, Khan W, Godugu C. Cytotoxicity of nanomaterials: nanotoxicology to address the safety concerns of nanoparticles. *Pharm Nanotechnol*. 2017;6(1):3–16.
20. Heurtault B, Saulnier P, Pech B, Proust JE, Benoit JP. A novel phase inversion-based process for the preparation of lipid nanocarriers. *Pharm Res*. 2002;19(6):875–880.
21. Roger E, Lagarce F, Benoit JP. The gastrointestinal stability of lipid nanocapsules. *Int J Pharm*. 2009;379(2):260–265.
22. Roger E, Lagarce F, Benoit JP. Development and characterization of a novel lipid nanocapsule formulation of Sn38 for oral administration. *Eur J Pharm Biopharm*. 2011;79(1):181–188.
23. Groo AC, Saulnier P, Gimel JC, et al. Fate of paclitaxel lipid nanocapsules in intestinal mucus in view of their oral delivery. *Int J Nanomedicine*. 2013;8:4291–4302.
24. Roger E, Lagarce F, Garcion E, Benoit JP. Lipid nanocarriers improve paclitaxel transport throughout human intestinal epithelial cells by using vesicle-mediated transcytosis. *J Control Release*. 2009;140(2):174–181.
25. Roger E, Lagarce F, Garcion E, Benoit JP. Reciprocal competition between lipid nanocapsules and P-gp for paclitaxel transport across Caco-2 cells. *Eur J Pharm Sci*. 2010;40(5):422–429.
26. Le Roux G, Moche H, Nieto A, Benoit JP, Nesslany F, Lagarce F. Cytotoxicity and genotoxicity of lipid nanocapsules. *Toxicol In Vitro*. 2017;41:189–199.
27. Maupas C, Moulari B, Beduneau A, Lamprecht A, Pellequer Y. Surfactant dependent toxicity of lipid nanocapsules in HaCaT cells. *Int J Pharm*. 2011;411(1–2):136–141.
28. Peltier S, Oger JM, Lagarce F, Couet W, Benoit JP. Enhanced oral paclitaxel bioavailability after administration of paclitaxel-loaded lipid nanocapsules. *Pharm Res*. 2006;23(6):1243–1250.
29. Ramadan A, Lagarce F, Tessier-Marteau A, et al. Oral fondaparinux: use of lipid nanocapsules as nanocarriers and in vivo pharmacokinetic study. *Int J Nanomedicine*. 2011;6:2941–2951.
30. Eissa MM, El-Moslemany RM, Ramadan AA, Amer EI, El-Azzouni MZ, El-Khordagui LK. Miltefosine lipid nanocapsules for single dose oral treatment of schistosomiasis mansoni: a preclinical study. *PLoS One*. 2015;10(11):e0141788.
31. Olliaro P, Delgado-Romero P, Keiser J. The little we know about the pharmacokinetics and pharmacodynamics of praziquantel (racemate and R-enantiomer). *J Antimicrob Chemother*. 2014;69(4):863–870.
32. Yang L, Geng YH, Li H, Zhang Y, You JS, Chang YY. Enhancement the oral bioavailability of praziquantel by incorporation into solid lipid nanoparticles. *Pharmazie*. 2009;64(2):86–89.
33. Xie SY, Pan BL, Wang M, et al. Formulation, characterization and pharmacokinetics of praziquantel-loaded hydrogenated castor oil solid lipid nanoparticles. *Nanomedicine*. 2010;5(5):693–701.
34. Mourao SC, Costa PI, Salgado HRN, Gremiao MPD. Improvement of antischistosomal activity of praziquantel by incorporation into phosphatidylcholine-containing liposomes. *Int J Pharm*. 2005;295(1–2):157–162.

35. Frezza TF, Gremiao MPD, Zanotti-Magalhaes EM, Magalhaes LA, de Souza ALR, Allegretti SM. Liposomal-praziquantel: efficacy against *Schistosoma mansoni* in a preclinical assay. *Acta Trop*. 2013;128(1):70–75.
36. Cong Z, Shi Y, Peng X, et al. Design and optimization of thermosensitive nanoemulsion hydrogel for sustained-release of praziquantel. *Drug Dev Ind Pharm*. 2017;43(4):558–573.
37. Peters PA, Warren KS. A rapid method of infecting mice and other laboratory animals with *Schistosoma mansoni*: subcutaneous injection. *J Parasitol*. 1969;55(3):558.
38. Smithers SR, Terry RJ. The infection of laboratory hosts with cercariae of *Schistosoma mansoni* and the recovery of the adult worms. *Parasitology*. 1965;55(4):695–700.
39. Figueiro F, de Oliveira CP, Rockenbach L, et al. Pharmacological improvement and preclinical evaluation of methotrexate-loaded lipid-core nanocapsules in a glioblastoma model. *J Biomed Nanotechnol*. 2015;11(10):1808–1818.
40. Webster JP, Molyneux DH, Hotez PJ, Fenwick A. The contribution of mass drug administration to global health: past, present and future. *Philos Trans R Soc Lond B Biol Sci*. 2014;369(1645):20130434.
41. Muchirah PJ, Yole D, Kutima H, Waihenya R, Muna K, John M. Determination of effective praziquantel dose in different mouse strains: BALB/C and swiss mice in treatment of *Schistosoma mansoni*. *J Clin Immnunol Immunopathol Res*. 2012;4(2):12.
42. Carbone C, Musumeci T, Lauro MR, Puglisi G. Eco-friendly aqueous core surface-modified nanocapsules. *Colloids Surf B Biointerfaces*. 2015;125:190–196.
43. Mally M, Peterlin P, Svetina S. Partitioning of oleic acid into phosphatidylcholine membranes is amplified by strain. *J Phys Chem B*. 2013;117(40):12086–12094.
44. Niu Z, Tedesco E, Benetti F, et al. Rational design of polyarginine nanocapsules intended to help peptides overcoming intestinal barriers. *J Control Release*. 2017;263:4–17.
45. Talegaonkar S, Azeem A, Ahmad FJ, Khar RK, Pathan SA, Khan ZI. Microemulsions: a novel approach to enhanced drug delivery. *Recent Pat Drug Deliv Formul*. 2008;2(3):238–257.
46. Lin J, Mori F. Effect of polar components on phase inversion temperatures in systems containing nonionic surfactants and nonpolar oils. *J Korean Ind Eng Chem*. 1994;5(2):274–284.
47. Pensel PE, Ullio Gamboa G, Fabbri J, et al. Cystic echinococcosis therapy: albendazole-loaded lipid nanocapsules enhance the oral bioavailability and efficacy in experimentally infected mice. *Acta Trop*. 2015;152:185–194.
48. Zheng XS, Duan CZ, Xiao ZD, Yao BA. Transdermal delivery of praziquantel: effects of solvents on permeation across rabbit skin. *Biol Pharm Bull*. 2008;31(5):1045–1048.
49. Xiao SH, Shen BG, Chollet J, Tanner M. Tegumental changes in 21-day-old *Schistosoma mansoni* harboured in mice treated with artemether. *Acta Trop*. 2000;75(3):341–348.
50. El-Moslemany RM, Eissa MM, Ramadan AA, El-Khordagui LK, El-Azzouni MZ. Miltefosine lipid nanocapsules: intersection of drug repurposing and nanotechnology for single dose oral treatment of prepatent schistosomiasis mansoni. *Acta Trop*. 2016;159:142–148.
51. Gamboa GV, Palma SD, Lifschitz A, et al. Ivermectin-loaded lipid nanocapsules: toward the development of a new antiparasitic delivery system for veterinary applications. *Parasitol Res*. 2016;115(5):1945–1953.
52. Pabla D, Akhlaghi F, Zia H. Intestinal permeability enhancement of levothyroxine sodium by straight chain fatty acids studied in MDCK epithelial cell line. *Eur J Pharm Sci*. 2010;40(5):466–472.
53. El-Faham MH, Eissa MM, Igetei JE, et al. Treatment of *Schistosoma mansoni* with miltefosine in vitro enhances serological recognition of defined worm surface antigens. *PLoS Negl Trop Dis*. 2017;11(8):e0005853.
54. Kato K, Walde P, Koine N, et al. Temperature-sensitive nonionic vesicles prepared from Span 80 (sorbitan monooleate). *Langmuir*. 2008;24(19):10762–10770.
55. Abla N, Keiser J, Vargas M, Reimers N, Haas H, Spangenberg T. Evaluation of the pharmacokinetic-pharmacodynamic relationship of praziquantel in the *Schistosoma mansoni* mouse model. *PLoS Negl Trop Dis*. 2017;11(9):e0005942.
56. Serrano DR, Lalatsa A, Dea-Ayuela MA, et al. Oral particle uptake and organ targeting drives the activity of amphotericin B nanoparticles. *Mol Pharm*. 2015;12(2):420–431.
57. Roger E, Gimel JC, Bensley C, Klymchenko AS, Benoit JP. Lipid nanocapsules maintain full integrity after crossing a human intestinal epithelium model. *J Control Release*. 2017;253:11–18.
58. Tobio M, Sanchez A, Vila A, et al. The role of PEG on the stability in digestive fluids and in vivo fate of PEG-PLA nanoparticles following oral administration. *Colloids Surf B Biointerfaces*. 2000;18(3–4):315–323.
59. Groo AC, Mircheva K, Bejaud J, et al. Development of 2D and 3D mucus models and their interactions with mucus-penetrating paclitaxel-loaded lipid nanocapsules. *Pharm Res*. 2014;31(7):1753–1765.
60. Cury-Boaventura MF, Gorjao R, de Lima TM, Newsholme P, Curi R. Comparative toxicity of oleic and linoleic acid on human lymphocytes. *Life Sci*. 2006;78(13):1448–1456.
61. Eibl H, Unger C, Fleer EAM, Kim DJ, Berger MR, Nagel GA. Hexadecylphosphocholine, a new antineoplastic agent: cytotoxic properties in leukaemic cells. *J Cancer Res Clin Oncol*. 1986;111:S24.
62. Unger C, Damenz W, Fleer EA, et al. Hexadecylphosphocholine, a new ether lipid analogue. Studies on the antineoplastic activity in vitro and in vivo. *Acta Oncol*. 1989;28(2):213–217.
63. de Souza AL, Andreani T, de Oliveira RN, et al. In vitro evaluation of permeation, toxicity and effect of praziquantel-loaded solid lipid nanoparticles against *Schistosoma mansoni* as a strategy to improve efficacy of the schistosomiasis treatment. *Int J Pharm*. 2014;463(1):31–37.